AGU PUBLICATIONS

Geophysical Research Letters

RESEARCH LETTER
10.1002/2014GL062956

Key Points:
- Observed anomaly were the manifestation of a known teleconnection
- Perturbations were forced by the Pacific SST and Arctic sea ice
- Natural variability and anthropogenic warming both contributed to the event

Supporting Information:
- Table S1 and Figures S1–S3

Correspondence to:
H.-H. Hsu,
hhhsu@gate.sinica.edu.tw

Citation:
Lee, M.-Y., C.-C. Hong, and H.-H. Hsu (2015), Compounding effects of warm sea surface temperature and reduced sea ice on the extreme circulation over the extratropical North Pacific and North America during the 2013–2014 boreal winter, *Geophys. Res. Lett.*, *42*, 1612–1618, doi:10.1002/2014GL062956.

Received 25 DEC 2014
Accepted 13 FEB 2015
Accepted article online 16 FEB 2015
Published online 13 MAR 2015

Compounding effects of warm sea surface temperature and reduced sea ice on the extreme circulation over the extratropical North Pacific and North America during the 2013–2014 boreal winter

Ming-Ying Lee[1], Chi-Cherng Hong[2], and Huang-Hsiung Hsu[3]

[1]Central Weather Bureau, Taipei, Taiwan, [2]Department of Earth and Life, University of Taipei, Taipei, Taiwan, [3]Research Center for Environmental Changes, Academia Sinica, Taipei, Taiwan

Abstract Unprecedented atmospheric circulations with extreme weather were observed in the extratropical Northern Hemisphere during the winter of 2013–2014. The anomalous circulations were the manifestation of the Pacific pattern or the North Pacific Oscillation/Western Pacific pattern but with extremely large amplitude. Simulation results suggest that the anomalous atmospheric circulations were constructively induced by anomalous sea surface temperature in the tropical Pacific and extratropical North Pacific, as well as the low sea ice concentration in the Arctic. Natural variability played a major role in inducing the anomaly pattern, whereas the anomalously warm sea surface temperature and low Arctic sea ice concentration in the Bering Sea contributed to the intensity. If the anthropogenic warming has a significant impact on causing the synchronization of the aforementioned anomalies in sea surface temperature and sea ice concentration and this trend continues, severe winters similar to that in 2013–2014 may occur more frequently in the future.

1. Introduction

Many extreme weather and climatic events occurred in the extratropical Northern Hemisphere in the boreal winter of 2013–2014 (e.g., an unusually warm winter in Alaska and the Bering Sea, wildfires and severe drought in California, as well as severe snowstorms and cold temperature in eastern North America). In Europe, while most countries experienced a milder winter, the United Kingdom experienced its wettest winter on record. The geopotential height at 500 hPa (H500) and the air temperature at 850 hPa (T850) (Figure 1a) revealed the anomalous circulation causing these extreme events. An extremely anomalous ridge (exceeding the 95th percentile corresponding to the period from 1948–1949 to 2013–2014) was observed over the west coast of North America, Alaska, and the high-latitude North Pacific, extending into the Arctic. By contrast, negative height anomalies were observed over eastern North America and the extratropical North Atlantic. To the south of these negative anomalies, an unprecedented subtropical height existed over the subtropical North Atlantic. As expected, positive and negative T850 anomalies were associated with the positive and negative H500 anomalies. Most of the aforementioned anomalies exceeded either the 95th or 5th percentile, suggesting that the winter of 2013–2014 was among the most severe winters since the late 1940s.

Low sea ice concentration (SIC) in the Arctic and positive sea surface temperature (SST) anomaly in the tropical western Pacific (TWP) have been found to induce anomalous atmospheric circulation in the northern extratropics [*Francis and Vavrus*, 2012; *Mori et al*., 2014; *Frankignoul et al*., 2014; *Ding et al*., 2014]. Regarding the recent 2013–2014 event, *Palmer* [2014] argued that according to past studies, the warming in the TWP might have excited Rossby waves that caused the anomalous extratropical circulation. *Wang et al*. [2014] proposed that an abnormal ridge observed over the eastern North Pacific in the winter of 2013–2014 was correlated with a type of El Niño–Southern Oscillation precursor occurring in the TWP. In addition, *Wang and Schubert* [2014] and *Funk et al*. [2014] have indicated that the extreme drought in California in 2013–2014 and the corresponding anomalous ridge were closely related to the extremely warm SST in the extratropical North Pacific (ExtraNP). Whether the warming trend caused the severe drought has also been discussed. Some studies [e.g., *Palmer*, 2014; *Wang et al*., 2014; *Swain et al*., 2014] have suggested the possible contribution of anthropogenic warming, whereas others [*Wang and Schubert*, 2014; *Funk et al*., 2014] have indicated no appreciable contribution. *Wallace et al*. [2014] reasoned that similar cold events occurred in

©2015. American Geophysical Union. All Rights Reserved.

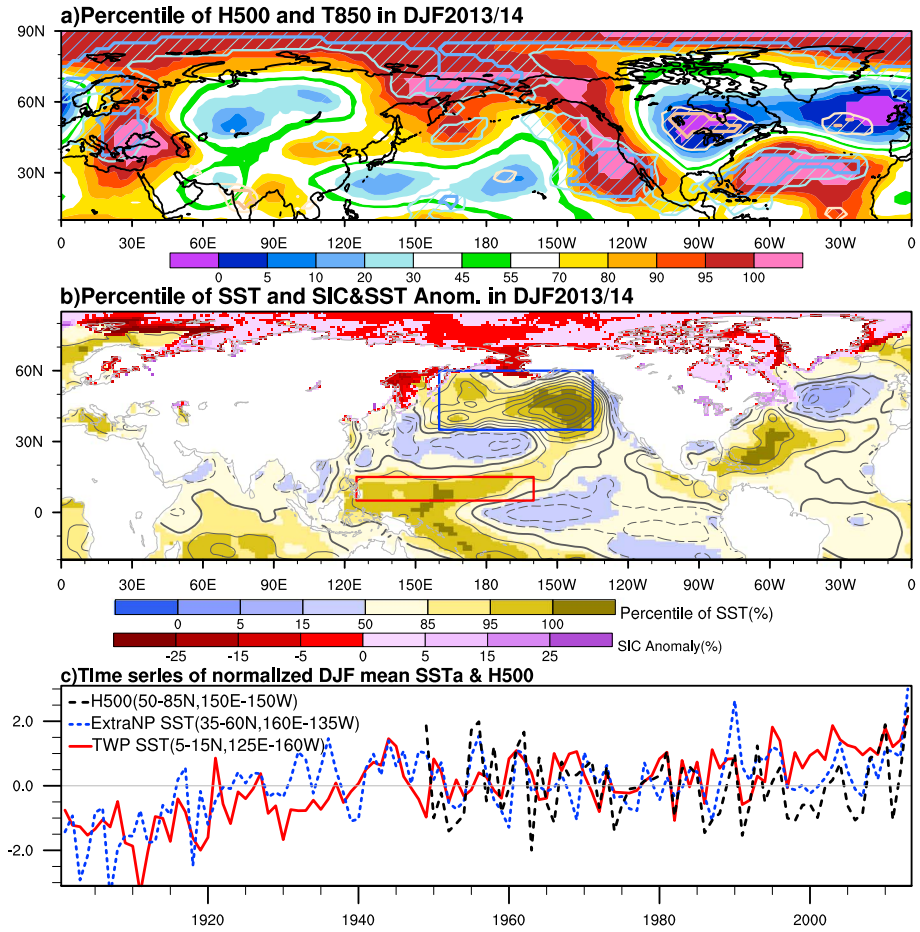

Figure 1. (a) Percentiles of H500 (color shaded) and T850 (hatched with 0%, 5%, 95%, and 100% contours) in DJF 2013–2014. Percentiles of (b) SST (color shaded), SICa (in percentage, red and purple color shading), and SSTa (in Kelvin; contour interval: 0.3 K; solid, dashed, and thickened lines denote positive, negative, and zero values, respectively) in DJF 2013–2014. (c) Time series of the normalized SST averaged over the TWP (area marked by the red line in Figure 1b), the ExtraNP (area marked by the blue line in Figure 1b), and H500 averaged over (50°–85°N, 150°E–150°W) in DJF 2013–2014.

the past and cautioned against attributing the event to anthropogenic warming. In this paper, we present another perspective of this exceptional winter by conducting circulation diagnostics and numerical simulations with various lower boundary forcings to demonstrate that similar anomalous atmospheric circulation patterns had repeatedly occurred in the past and that the compounding effect of the anomalous SST in the Pacific as well as the low SIC in the Arctic are the likely causes of the unusual winter of 2013–2014.

2. Data, Model, and Analysis Procedure

The observational data used in this study are monthly atmospheric fields from National Centers for Environmental Prediction/National Center for Atmospheric Research Reanalysis I [*Kalnay et al.*, 1996], SST data from the National Oceanic and Atmospheric Administration (NOAA) Extended Reconstructed sea surface temperature (version 3b) [*Smith et al.*, 2007], and SIC data from the NOAA Optimum Interpolation Sea Surface Temperature (version 2) [*Reynolds et al.*, 2002].

The European Centre Hamburg Atmosphere Model (ECHAM5, version 5), which is an atmospheric general circulation model [*Roeckner et al.*, 2003] with T42 horizontal resolution and 31 vertical sigma levels, is used in the numerical experiments to determine the relative influence of the SST anomaly (SSTa) in various regions and the SIC anomaly (SICa) in the Northern Hemisphere (NH).

©2015. American Geophysical Union. All Rights Reserved.

3. Analysis Results

The SSTa for December to February (DJF) 2013–2014 shown in Figure 1b reveals a moderate amplitude in the tropical eastern Pacific (TEP). By contrast, an SSTa above the 95th percentile existed in most of the TWP. Another unprecedented warm SST is observed in the ExtraNP ($SST_{ExtraNP}$), particularly in the eastern region, where an SSTa above 95% was observed. The three time series for the SSTa in the TWP and ExtraNP (SST_{TWP} and $SST_{ExtraNP}$, respectively; regions marked in Figure 1b) and H500 over the ExtraNP and Arctic ($H500_{ExtraNP}$; 50°N–85°N, 150°E–150°W) shown in Figure 1c indicate that all three indices show record-breaking amplitudes in the boreal winter of 2013–2014, with the magnitude of the $SST_{ExtraNP}$ approaching three standard deviations. The interannual fluctuations in the $SST_{ExtraNP}$ and $H500_{ExtraNP}$ indices (blue and black lines in Figure 1c) are significantly correlated (0.59; 99% confidence level). In addition to the extremely warm SST, a significantly reduced SIC near the Arctic was observed in DJF 2013–2014 (Figure 1b). The coexistence of the SSTa, SICa, anomalous ridges and troughs, and warmth and coldness raises the following questions, which are addressed in this letter: (1) Did the anomalous lower boundary conditions such as the SSTa and SICa serve as forcing to induce or enhance the observed anomalous atmospheric circulation (despite some of the observed SSTa and SICa being initially induced by the anomalous atmospheric flow)? (2) What were the relative contributions of the various boundary forcings?

To verify the relationship between the boundary forcings and the unusual atmospheric circulation anomalies in the winter of 2013–2014, empirical orthogonal function (EOF) analysis is applied to the H500 poleward of 20°N for data corresponding to the period 1981–1982 to 2013–2014. The first EOF explaining 19.6% of the total variance resembles the Artic Oscillation (AO) [*Thompson and Wallace*, 1998]. However, the weak AO index (approximately 0.17) in DJF 2013–2014 suggests that the AO was not strong in the 2013–2014 event. The second EOF ($EOF2_{H500}$) explaining 14.2% of the total variance exhibited a quadrupole structure over the North Pacific, North America, and the North Atlantic (Figure 2a). This pattern and the anomalies in DJF 2013–2014 are highly similar. The pattern also resembles the Pacific pattern identified by *Hsu and Wallace* [1985] and the North Pacific Oscillation/Western Pacific (NPO/WP) pattern identified by *Linkin and Nigam* [2008]. $EOF2_{H500}$ is significantly correlated with an SSTa pattern (i.e., a positive correlation in the TWP and ExtraNP, as well as a negative correlation in the TEP, Figure 2b) in the Pacific basin, which resembles the SSTa observed in DJF 2013–2014. Figures 2a and 2b are derived from the nondetrended data. Similar results are obtained when detrended data are used for calculation. Figure 2c shows that the warming trend may enhance the SST and SIC, but its influence on EOF2 (i.e., principal component 2, PC2) is negligible.

Applying EOF analysis to the SIC over the high-latitude North Pacific reveals the second EOF ($EOF2_{sic}$) with a uniformly reduced SIC in the Bering Sea and the Sea of Okhotsk, resembling the observed SICa in DJF 2013–2014 (Figure S1a in the supporting information). The correlation map of H500 regressed on $EOF2_{sic}$ (Figure S1b) resembles the structure of $EOF2_{H500}$ and the observed H500 anomaly in DJF 2013–2014, particularly the positive correlation over Alaska and the Bering Sea. This high similarity between the H500 anomaly patterns derived from various approaches suggests that the observed anomalous atmospheric circulation is a manifestation of a known and repeatedly appearing teleconnection pattern, which is well correlated with the Pacific SST and Arctic SIC.

The close relationship among $EOF2_{H500}$, the SSTa, and the SICa suggests that the observed atmospheric anomalies might have been influenced, at least partially, by the SSTa and SICa. Although the correlations (0.3–0.4) between $EOF2_{H500}$ and the SST and SIC anomalies are statistically significant, they are not particularly strong, indicating that the SSTa and SICa are not always closely associated with the atmospheric anomaly represented by $EOF2_{H500}$. This raises a crucial question: Why did the $EOF2_{H500}$-like anomaly reach such large amplitude in DJF 2013–2014?

Figure 2c show the time series of $EOF2_{H500}$ and four surface indices: the SSTa indices of TEP, TWP, ExtraNP, and the NH SIC (north of 45°N; SIC_{NH}). The temporal correlation coefficients for $EOF2_{H500}$ with SIC_{NH}, $SST_{ExtraNP}$, SST_{TWP}, and SST_{TEP} were 0.51, 0.62, 0.58, and 0.52, respectively (all exceed the 99% confidence level). All four indices are anomalously positive, with three of them exceeding one standard deviation in DJF 2013–2014. We hypothesize that the extremely warm SST in the TWP and the extratropical North Pacific, as well as the extremely low SIC in the Northern Hemisphere, jointly led to the extremely anomalous atmospheric circulation in the North Pacific, North America, and the North Atlantic in DJF 2013–2014.

©2015. American Geophysical Union. All Rights Reserved.

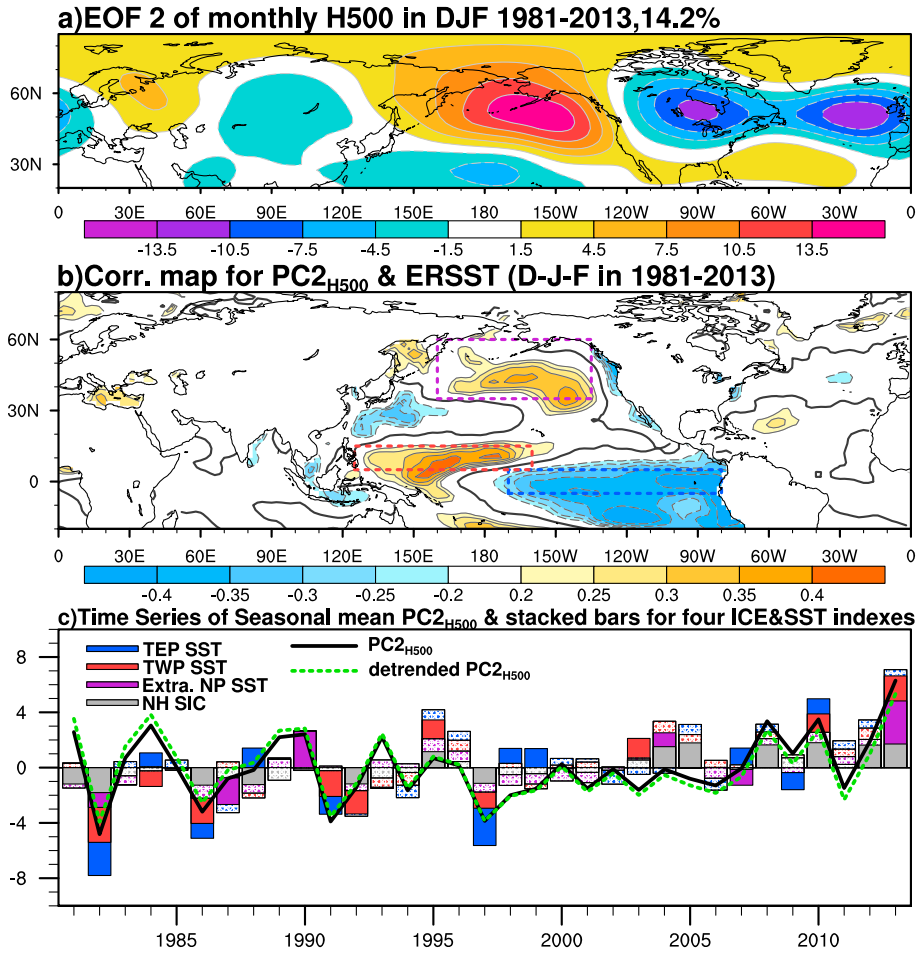

Figure 2. (a) Second EOF of monthly H500 explaining 14.2% of the variance in DJF 1981–2013. (b) Correlation map between the second principal component of H500 ($PC2_{H500}$) and the SST in DJF 1981–2013. (c) Time series of the seasonal mean of $PC2_{H500}$ for the original (black line) and detrended (green dashed line) H500, and stacked bars for the four normalized indices: the SST averaged over the TEP (blue bars), TWP (red bars), ExtraNP (purple bars), and the SIC averaged over the region poleward of 45°N (grey bars). The selected areas are marked in Figure 2b. The TEP SST and NH SIC were multiplied by −1. The stacked bars in Figure 2c are filled with dots where the magnitude is less than one standard deviation.

4. Numerical Experiments

To test our hypothesis, we conduct a series of numerical experiments using ECHAM5 (Table 1 in the supporting information) to simulate the atmospheric circulation in DJF 2013–2014 under the forcing of the observed SSTa and Arctic SICa. Each experiment includes 10 member simulations from October to February, with the observed initial conditions set to correspond to 1–10 October 2013. Figure S2 (supporting information) shows the domains for the prescribed SSTa in the ExtraNP experiment ($ExtraNP_{run}$), TWP experiment (TWP_{run}), TEP experiment (TEP_{run}), and Pacific experiment ($Pacific_{run}$). The observed climatological monthly SST is prescribed outside the chosen domains. The observed SIC north of 45°N is prescribed in *Pacific* + SIC_{run} and *TWP* + SIC_{run} to examine the effect of the Arctic SICa. An additional experiment, the Bering Sea and Sea of Okhotsk SIC experiment (BO SIC_{run}), reveals the influence of the local SICa in these two regional seas. To account for the potential effect of regime shift occurring around 1998, the 1998–2010 period is defined as the reference period for conducting control simulations and defining the climatological mean and anomaly. The differences between the aforementioned experiments and the control experiment are compared with the observed anomalies to evaluate the model responses to the prescribed boundary forcings.

The most realistic response to the prescribed forcing among all experiments is obtained in Pacific + SIC_{run}, which includes forcings from all SSTa's north of 30°S in the Pacific and the SICa in the entire Arctic. The simulation captures most of the characteristics for the 500 hPa height over the North Pacific and North

©2015. American Geophysical Union. All Rights Reserved.

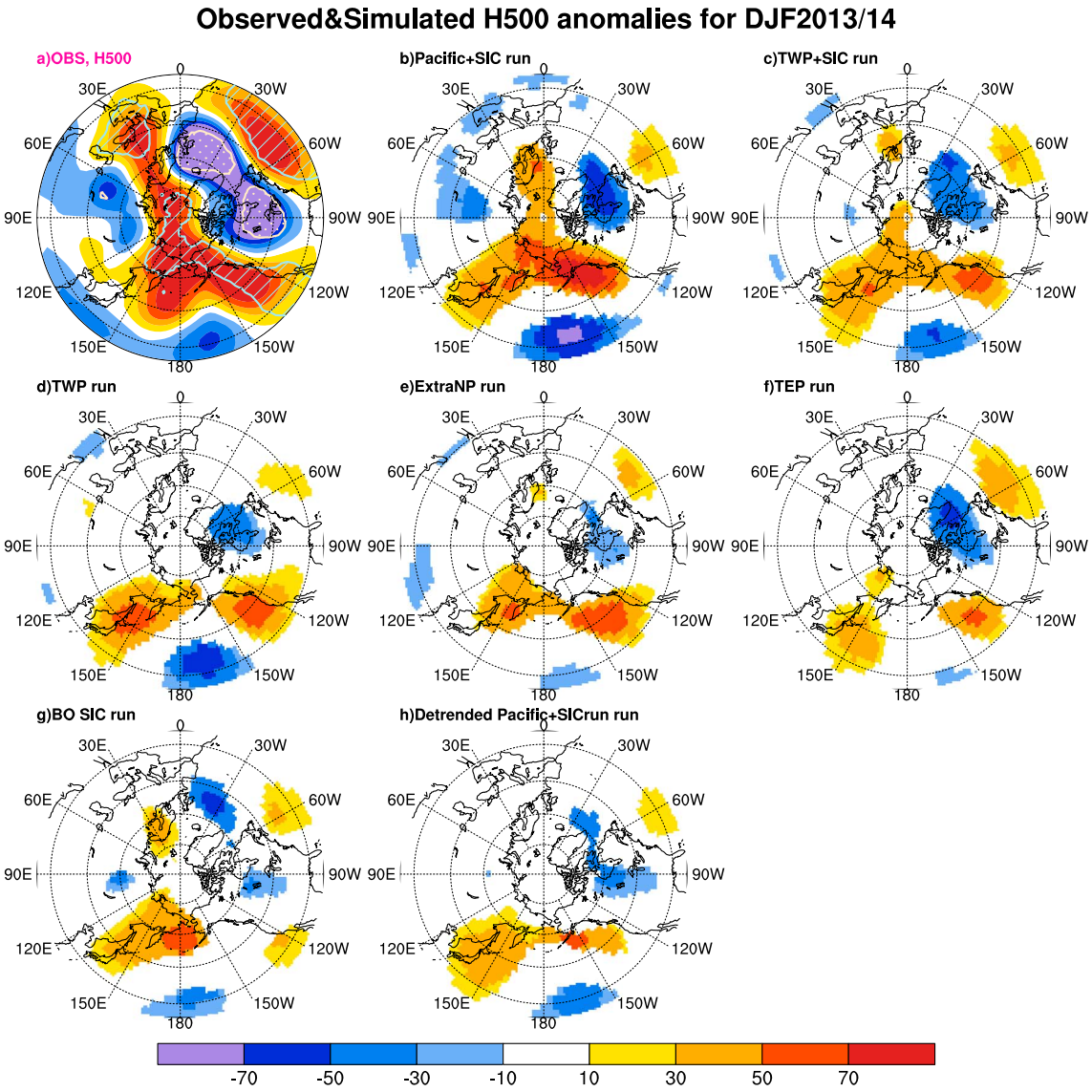

Figure 3. Observed and simulated anomalous fields for DJF 2013–2014. (a) Observed H500 anomaly. (b–g) Same as in Figure 3a but for the simulated H500 in the Pacific + SICrun, TWP + SICrun, TWPrun, ExtraNPrun, TEPrun, BO SICrun, and detrended Pacific + SIC run. The hatching and dots in Figure 3a denote values exceeding the 95th and 5th percentiles, respectively. The shading in the simulated fields represents anomalies above the 90% confidence level from the 10 member ensemble simulations.

America, and even some features over Europe (Figures 3a and 3b). Both TWP + SIC_{run} and TWP_{run} produced results similar to those of Pacific + SIC_{run}, but with slightly weaker amplitudes (Figures 3c and 3d), particularly over the Eurasian Continent and the Arctic. ExtraNPrun (Figure 3e) and the contrast among the three aforementioned experiments demonstrate that, although the ExtraNP-SSTa might initially be induced by atmospheric anomalies, it can exert a positive effect on the anomalies to enhance the positive height anomaly over the Sea of Okhotsk and the wave-like pattern from the eastern North Pacific to the North Atlantic. This wave-like pattern, which is the dominant anomalous circulation that led to the abnormal weather and climatic events in the North Pacific/North America region in DJF 2013–2014, can also be forced by positive and negative SSTa's in the TWP (i.e., TWP_{run}, Figure 3d) and TEP (i.e., TEP_{run}, Figure 3f)), respectively. BO SIC_{run} suggests that the low SIC in the Bering Sea and the Sea of Okhotsk contributes most significantly to the anomalous height over the Bering Sea and also forces a far-field response similar to the observed anomaly (except for the positive anomaly off the west coast of North America) (Figure 3g).

These results indicate that the observed SSTa in various parts of the Pacific can force a wave-like pattern similar to the observed perturbation, and the reduced SIC, particularly in the Bering Sea, can enhance the

©2015. American Geophysical Union. All Rights Reserved.

perturbation at high latitudes. These forcings functioned jointly in DJF 2013–2014 and are likely to have caused the observed extreme event. Our hypothesis formulated based on observation is supported by the series of numerical simulations presented here.

5. Summary and Discussion

This letter explores, through observational data diagnostics and atmospheric general circulation simulations, the possible mechanisms leading to the extremely anomalous atmospheric circulation and warmth and coldness over the North Pacific and North America region during December–February 2013–2014. The observed anomalies are the manifestation of the second empirical orthogonal function for the 500 hPa geopotential height, which exhibits the characteristics of the Pacific pattern [*Hsu and Wallace*, 1985] and the North Pacific Oscillation/Western Pacific pattern [*Linkin and Nigam*, 2008]. The occurrence of the anomalies is not rare. The uniqueness of the anomalies lies in their extremely high amplitude.

The results of a series of numerical experiments confirm our hypothesis that the anomalously warm sea surface temperature in the tropical Pacific and the extratropical North Pacific and the extremely low sea ice concentration in the Arctic, particularly in the Bering Sea, constructively induced the anomalous atmospheric circulation over the North Pacific, North America, and the North Atlantic in December–February 2013–2014. Although the negative sea surface temperature anomaly in the tropical eastern Pacific is not particularly strong in a statistical sense, our simulation reveals a wave-like response as strong as that in other simulations. We hypothesize that the negative sea surface temperature anomaly is located to the south of the starting location of the wave-like pattern and likely forces the wave-like perturbation more efficiently. Therefore, the negative sea surface temperature anomaly in the tropical eastern Pacific should also be considered as one of the contributing forcings. This wave-like pattern across North America is forced by multiple boundary forcings. All simulations forced by the anomalous sea surface temperatures in the tropical western and eastern Pacific and the extratropical North Pacific reproduce the observed upper tropospheric divergence anomaly over the central extratropical North Pacific, which possibly functions as a Rossby wave source [*Sardeshmukh and Hoskins*, 1988] anomaly, inducing the wave-like pattern propagating downstream from the North Pacific to the North Atlantic (Figure S3). The existence of this feature may explain how various boundary forcings constructively contributed to the observed anomalous circulation in December–February 2013–2014.

The constructive synchronization of these large-amplitude forcings is unique to the boreal winter 2013–2014. Similar synchronization of forcings but with considerably lower amplitudes was appeared in the winters of 2010–2011 and 2012–2013 (Figure 2c), and the corresponding atmospheric anomalies are substantially weaker than those in 2013–2014 (not shown). Another synchronization of forcings (but in negative phase) occurring in 1982–1983 is associated with negative geopotential height anomalies. These forcings might have affected the winter climate in the North Pacific/North America region in the past (at least after 1981) but had never occurred constructively with such an extreme magnitude as that in December–February 2013–2014. Thus, this extreme event is partly attributable to natural variability. However, the rising sea surface temperature and reducing sea ice concentration over the past few decades may have an effect in amplifying the atmospheric anomalies. This hypothesis is supported by much weaker responses in a simulation forced by detrended sea surface temperature and sea ice concentration anomalies (Figure 3h). Note that the weakening in amplitude is statistically significant. This result suggests that the warming trend in recent decades might contribute at least partially to the extremity in the winter of 2013–2014. According to *Bindoff et al*. [2013], anthropogenic warming is partially responsible for the warming in the Pacific and the melting of the Arctic sea ice. If the anthropogenic warming has a significant impact on causing the synchronization of the aforementioned extreme sea surface temperature and sea ice concentration anomalies and this trend continues in the near future, severe winters similar to that in 2013–2014 may occur more frequently in the future.

Acknowledgments

The observational data used in this study are from the NOAA Earth System Research Laboratory (http://www.esrl.noaa.gov/psd/data/gridded/). Simulation data may be made available by contacting the corresponding author. This study was supported by the Ministry of Science and Technology, Taiwan, under grant NSC-100-2119-M-001-029-MY5 and NSC 101-2111-M133-001. The National Center for High-performance Computing provided computing resource for this study. The authors are grateful for the valuable comments of two anonymous reviewers.

The Editor thanks James Screen and an anonymous reviewer for their assistance evaluating this paper.

References

Bindoff, N. L., et al. (2013), Detection and attribution of climate change: From global to regional, in *Climate Change 2013: The Physical Science Basis. Contribution of Working Group I to the Fifth Assessment Report of the Intergovernmental Panel on Climate Change*, edited by T. F. Stocker et al., pp. 867–952, Cambridge Univ. Press, Cambridge, U. K., and New York.

Ding, Q., J. M. Wallace, D. S. Battisti, E. J. Steig, A. J. E. Gallant, H. J. Kim, and L. Geng (2014), Tropical forcing of the recent rapid Arctic warming in northeastern Canada and Greenland, *Nature*, *509*(7499), 209–212.

©2015. American Geophysical Union. All Rights Reserved.

Francis, J. A., and S. J. Vavrus (2012), Evidence linking Arctic amplification to extreme weather in mid-latitudes, *Geophys. Res. Lett.*, *39*, L06801, doi:10.1029/2012GL051000.
Frankignoul, C., N. Sennéchael, and P. Cauchy (2014), Observed atmospheric response to cold season sea ice variability in the Arctic, *J. Clim.*, *27*, 1243–1254.
Funk, C., A. Hoell, and A. Stone (2014), Examining the contribution of the observed global warming trend to the California droughts of 2012/13 and 2013/14, *Bull. Am. Meteorol. Soc.*, *95*, S11–S15.
Hsu, H.-H., and J. M. Wallace (1985), Vertical structure of wintertime teleconnection patterns in Northern Hemisphere, *J. Atmos. Sci.*, *42*, 1693–1710.
Kalnay, E., et al. (1996), The NCEP/NCAR 40-year reanalysis project, *Bull. Am. Meteorol. Soc.*, *77*, 437–471.
Linkin, M. E., and S. Nigam (2008), The North Pacific Oscillation–West Pacific teleconnection pattern: Mature-phase structure and winter impacts, *J. Clim.*, *21*, 1979–1997.
Mori, M., M. Watanabe, H. Shiogama, J. Inoue, and M. Kimoto (2014), Robust Arctic sea-ice influence on the frequent Eurasian cold winters in past decades, *Nat. Geosci.*, *7*, 869–873.
Palmer, T. (2014), Record-breaking winters and global climate change, *Science*, *344*(6186), 803–804, doi:10.1126/science.1255147.
Reynolds, R. W., N. A. Rayner, T. M. Smith, D. C. Stokes, and W. Wang (2002), An improved in situ and satellite SST analysis for climate, *J. Clim.*, *15*, 1609–1625.
Roeckner, E., et al. (2003), The atmospheric general circulation model ECHAM5. Part I: Model description Max Planck Institute for Meteorology *Rep. 349*, 127 pp.
Sardeshmukh, P. D., and B. J. Hoskins (1988), The generation of global rotation flow by steady idealized tropical divergence, *J. Atmos. Sci.*, *45*, 1228–1251.
Smith, T. M., R. W. Reynolds, T. C. Peterson, and J. Lawrimore (2007), Improvements to NOAA's historical merged land-ocean surface temperature analysis (1880–2006), *J. Clim.*, *21*, 2283–2296.
Swain, D. L., M. Tsiang, M. Haugen, D. Singh, A. Charland, B. Rajaratnam, and N. S. Diffenbaugh (2014), The extraordinary California drought of 2013/2014: Character, context, and the role of climate change, *Bull. Am. Meteorol. Soc.*, *95*(9), S3–S7.
Thompson, D. W. J., and J. M. Wallace (1998), The Arctic Oscillation signature in wintertime geopotential height and temperature fields, *Geophys. Res. Lett.*, *25*, 1297–1300, doi:10.1029/98GL00950.
Wallace, J. M., I. M. Held, D. W. J. Thompson, K. Trenberth, and J. E. Walsh (2014), Global warming and winter weather, *Science*, *343*, 729–730.
Wang, H., and S. Schubert (2014), Causes of the extreme dry conditions over California during early 2013, *Bull. Am. Meteorol. Soc.*, *95*, S7–S11.
Wang, S.-Y., L. Hipps, R. R. Gillies, and J.-H. Yoon (2014), Probable causes of the abnormal ridge accompanying the 2013–2014 California drought: ENSO precursor and anthropogenic warming footprint, *Geophys. Res. Lett.*, *41*, 3220–3226, doi:10.1002/2014GL059748.

©2015. American Geophysical Union. All Rights Reserved.